Ionics (2016) 22:1113–1123
DOI 10.1007/s11581-015-1627-4

ORIGINAL PAPER

Ionic conductivity and dielectric properties of potato starch-magnesium acetate biopolymer electrolytes: the effect of glycerol and 1-butyl-3-methylimidazolium chloride

M. F. Shukur[1] · **R. Ithnin**[1] · **M. F. Z. Kadir**[1]

Received: 27 August 2015 / Revised: 4 December 2015 / Accepted: 27 December 2015 / Published online: 15 January 2016

Abstract In the present work, the effect of glycerol and 1-butyl-3-methylimidazolium chloride (BmImCl) on the conductivity and dielectric properties of potato starch doped with magnesium acetate, $Mg(C_2H_3O_2)_2$-based electrolytes is studied. The electrolytes are prepared via solution cast technique. The interaction between the materials is proven by Fourier transform infrared (FTIR) analysis. Electrolyte with 20 wt.% $Mg(C_2H_3O_2)_2$ exhibits a room temperature conductivity of $(2.44 \pm 0.37) \times 10^{-8}$ S cm^{-1}. The addition of 30 wt.% glycerol to the best polymer-salt composition has further enhanced the conductivity to $(2.60 \pm 0.42) \times 10^{-6}$ S cm^{-1}. A conductivity of $(1.12 \pm 0.08) \times 10^{-5}$ S cm^{-1} has been achieved when 18 wt.% BmImCl is added to the best polymer-salt-plasticizer composition. From the loss tangent (tan δ) plot, the relaxation time (t_r) for selected electrolytes is determined. From transference number measurements, ions are found to be the dominant charge carriers.

Keywords Solid polymer electrolyte · Potato starch · Magnesium acetate · Conductivity · Dielectric properties

Introduction

Solid polymer electrolytes based on natural polymers are exciting prospects for use in electrochemical devices [1–3]. Natural polymers possess advantageous properties such as non-toxic, naturally degrade, and low production cost [4, 5]. Several natural polymers have been used as electrolyte's host, e.g., chitosan [3], agar [6], and starch [7]. Starch is a mixture of linear amylose (poly-α-1,4-D-glucopyranoside) and branched amylopectin (poly-α-1,4-D-glucopyranoside and α-1,6-D-glucopyranoside) [8]. A lot of solvents have been used to dissolve starch such as water [7, 9, 10], dimethylsulfoxide (DMSO) [11], and *N*-methylmorpholine-*N*-oxide (NMMO) [12, 13]. However, both DMSO and NMMO are poisonous and unrecyclable [14]. Thus, in this work, we used a water-based solvent to dissolve starch since water is the most abundant and greenest solvent on earth [14]. Starch is a hydrophilic material and can form a mechanically poor film [15, 16]. The mechanical strength and hydrophobicity of starch film can be improved by using acetic acid as the solvent [17, 18]. It is reported that when starch reacts with an acid, the water solubility of the starch granules is enhanced [19]. Tiwari et al. [10, 20] and Kumar et al. [21] have studied different types of starches as polymer hosts in electrolyte. According to Kumar et al. [21], morphology of potato starch is better in comparison with other starches.

Incorporation of salt to the polymer is an important feature to provide ions as the charge carriers. Lithium salts such as lithium hexafluorophosphate ($LiPF_6$) [22], lithium perchlorate ($LiClO_4$) [2], and lithium triflate ($LiCF_3SO_3$) [23] are commonly preferred in the studies on polymer electrolyte since lithium is the lightest of all metals and could provide the largest possible potential window [24]. However, electrochemical devices that use lithium-salt-based electrolyte have several disadvantages, such as high cost, difficulty in handling lithium electrodes, and safety hazard [25]. Magnesium salt appears to be a potential alternative to lithium salt. Magnesium is non-toxic, less reactive toward oxygen and water, may be handled safely in open air, and hazards are minimized [26].

The content of this paper was presented at the ICFMD 2015.

✉ M. F. Z. Kadir
mfzkadir@um.edu.my

[1] Centre for Foundation Studies in Science, University of Malaya, 50603 Kuala Lumpur, Malaysia

Various ways have been employed to improve the conductivity of solid polymer electrolytes which are incomparable to those of liquid electrolytes. The addition of plasticizers such as ethylene carbonate (EC) [27, 28], dimethylacetamide (DMA) [29], and dibutyl phthalate (DBP) [30] has been reported to enhance the conductivity. The most common plasticizers for starch-based films are polyols, such as glycerol [31]. The addition of glycerol to the starch-based electrolyte is reported to enhance the cation mobility which in turn increases the ionic conductivity [32]. Based on our previous work [33], the addition of glycerol in a starch-based electrolyte can assist the dissociation of salt by weakening the Coulombic force between anion and cation. The increase in the degree of salt dissociation increases the number density of ions which can lead to conductivity enhancement [28].

The incorporation of ionic liquids (ILs) to the polymer electrolytes is another alternative to enhance the ionic conductivity [34, 35]. Generally, ionic liquid consists of a large asymmetrical cation and a weakly coordinating inorganic or organic anion [35]. Ionic liquids have attracted attention due to their good chemical and electrochemical stability, non-flammability, and high ionic conductivity [36]. Ramesh et al. [9] reported that the incorporation of 1-butyl-3-methylimidazolium hexafluorophosphate ($BmImPF_6$) into starch-lithium hexafluorophosphate ($LiPF_6$)-based electrolyte increased the ambient temperature conductivity from $\sim 10^{-7}$ S cm^{-1} to $(1.47 \pm 0.02) \times 10^{-4}$ S cm^{-1}. In this work, starch-based electrolytes were doped with magnesium acetate, $Mg(C_2H_3O_2)_2$. The aim of this work is to investigate the effect of glycerol and 1-butyl-3-methylimidazolium chloride (BmImCl) on the conductivity and dielectric properties of the electrolytes.

Experimental

Electrolyte preparation

For the preparation of salted system, 2 g of potato starch (Sigma-Aldrich) was dissolved in 50 mL of 1 % acetic acid solvent (SYSTERM) at 80 °C for 20 min. After the solutions cooled to room temperature, different amounts of $Mg(C_2H_3O_2)_2$ (R&M Chemicals) were added and stirred at room temperature until complete dissolution. For the preparation of plasticized system, different amounts of glycerol (SYSTERM) were added to the highest conducting salted electrolyte solution and stirred at room temperature until complete dissolution. For the preparation of IL-based system, different amounts of BmImCl (Sigma-Aldrich) were added to the highest conducting plasticized electrolyte solutions and stirred at room temperature until complete dissolution. All solutions were then poured into different plastic Petri dishes and left to dry at room temperature to form films. The dried films were stored in a desiccator filled with silica gel desiccants for further drying process. The compositions of all electrolytes in salted, plasticized, and IL-based systems are tabulated in Tables 1, 2, and 3, respectively.

Electrolyte characterization

The interactions of polymer-salt, polymer-salt-plasticizer, and polymer-salt-plasticizer-IL were determined by Fourier transform infrared (FTIR) spectroscopy using the Spotlight 400 Perkin-Elmer spectrometer in the wavenumber range of 450–4000 cm^{-1} at a resolution of 1 cm^{-1}. The measurements were carried out at room temperature.

Electrochemical impedance spectroscopy (EIS) measurements were conducted using HIOKI 3532-50 LCR HiTESTER in the frequency range of 50 Hz to 1 MHz at room temperature. The electrolytes were placed between two stainless steel blocking disc electrodes under spring pressure. The values of bulk resistance (R_b) were determined from the Cole-Cole plots obtained from the EIS measurements. Conductivity (σ) was calculated using the following equation:

$$\sigma = \frac{d}{R_b A} \tag{1}$$

where d is the electrolyte's thickness and A is the contact area of electrode and electrolyte.

The transference number of ion (t_{ion}) was measured using DC polarization method [37]. A cell consisting of the highest conducting electrolyte sandwiched by two stainless steel blocking electrodes was polarized using V&A Instrument DP3003 digital DC power supply at 0.50 V. The DC current was monitored as a function of time. The measurement was done at room temperature.

Results and discussion

FTIR analysis

FTIR spectra of electrolytes in the salted system in the hydroxyl band region are shown in Fig. 1a. The hydroxyl band peak

Table 1 Composition and designation of electrolytes in the salted system

Starch/$Mg(C_2H_3O_2)_2$ composition (wt.%)	Designation
100:0	S0
95:5	S5
90:10	S10
85:15	S15
80:20	S20
75:25	S25
70:30	S30

Table 2 Composition and designation of electrolytes in the plasticized system

S20/glycerol composition (wt.%)	Designation
95:5	P5
90:10	P10
85:15	P15
80:20	P20
75:25	P25
70:30	P30
65:35	P35
60:40	P40

in the spectrum of S0 appears at 3312 cm^{-1}. The hydroxyl band peak appears at 3298 cm^{-1} in the spectrum of S5. The hydroxyl band peak is observed to appear at a lower wavenumber as the salt content increases up to 30 wt.%. From the literature [20, 38, 39], the band shift indicates the interaction between the polymer and salt. Thus, the shifting of hydroxyl band peak with increasing salt content proves that the cation (Mg^{2+}) of salt interacts with the oxygen atom of the hydroxyl group. The oxygen atoms in polymer have negatively charged electron pairs so that the positively charged cations can coordinate at such atoms [40]. This kind of interaction is called dative bond. According to Stygar et al. [41], although interaction between polymer and salt mainly occurs at the oxygen atom, other bands can also be affected. The FTIR spectra of electrolytes in the salted system in the region of 2800–2980 cm^{-1} are shown in Fig. 1b. A peak which is assigned to C–H stretching mode of starch appears at 2925 cm^{-1} in the spectrum of S0. The peak is observed to shift with the addition of salt. From our previous work [33], C–H stretching mode of corn starch has been shifted on addition of ammonium bromide (NH_4Br) which is comparable with the present result.

Figure 2 depicts the FTIR spectra of electrolytes in the salted system in the region of 955–1055 cm^{-1}. This region represents the anhydroglucose ring of O–C stretch [42]. In the spectrum of S0, the peak is located at 993 cm^{-1}. The peak is observed to shift with the addition of salt indicating the interaction between cation of salt and oxygen atom in anhydroglucose ring of starch.

FTIR spectra of electrolytes in the plasticized system in the hydroxyl band region are shown in Fig. 3. The hydroxyl band

Table 3 Composition and designation of electrolytes in the IL-based system

P30/BmImCl composition (wt.%)	Designation
95:5	B5
91:9	B9
88:12	B12
85:15	B15
82:18	B18

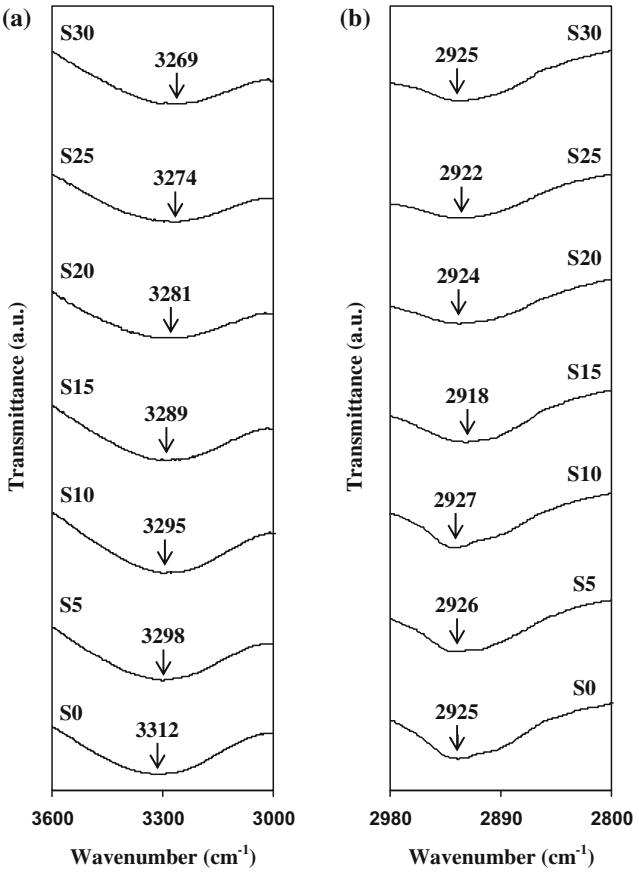

Fig. 1 FTIR spectra for electrolytes in the salted system in the wavenumber region of **a** 3000–3600 cm^{-1} and **b** 2800–2980 cm^{-1}

peak in the spectrum of P5 appears at 3276 cm^{-1}, which is lower than the hydroxyl band peak position of S20. As the glycerol content increases up to 30 wt.%, the hydroxyl band peak is observed to shift to a lower wavenumber. From a report by Yusof et al. [43], the hydroxyl band peak of starch-chitosan-ammonium iodide (NH_4I) has shifted to the lower wavenumber on addition of glycerol. The addition of glycerol promotes ion dissociation so that more ions interact with the polymer host at the hydroxyl band. Besides, glycerol is able to form hydrogen bonding with the polymer host [44]. These phenomena have been evidenced by the shifting of FTIR spectra in Fig. 3. The hydroxyl band peak has shifted back to the higher wavenumber in the spectra of P35 and P40. High concentration of plasticizer can lead to the decrease in amorphousness of electrolyte; thus, less ions interact with the polymer host [1]. It can be noted that the intensity of the hydroxyl band peak increases as the glycerol content increases. This result has further proven the interaction between Mg^{2+} cations and oxygen atoms in the hydroxyl band.

Another evidence of starch-$Mg(C_2H_3O_2)_2$-glycerol interaction can be observed in the region of 955–1055 cm^{-1} as shown in Fig. 4. The peak of anhydroglucose ring of O–C stretch in the spectrum of S20 is located at 997 cm^{-1}. The peak is observed to shift with the addition of glycerol. It can be inferred

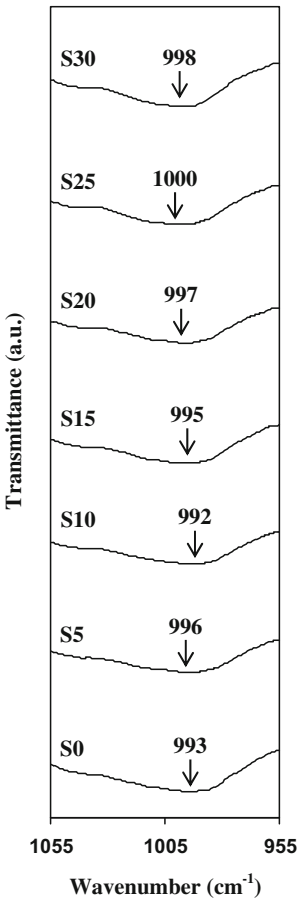

Fig. 2 FTIR spectra for electrolytes in the salted system in the wavenumber region of 955–1055 cm^{-1}

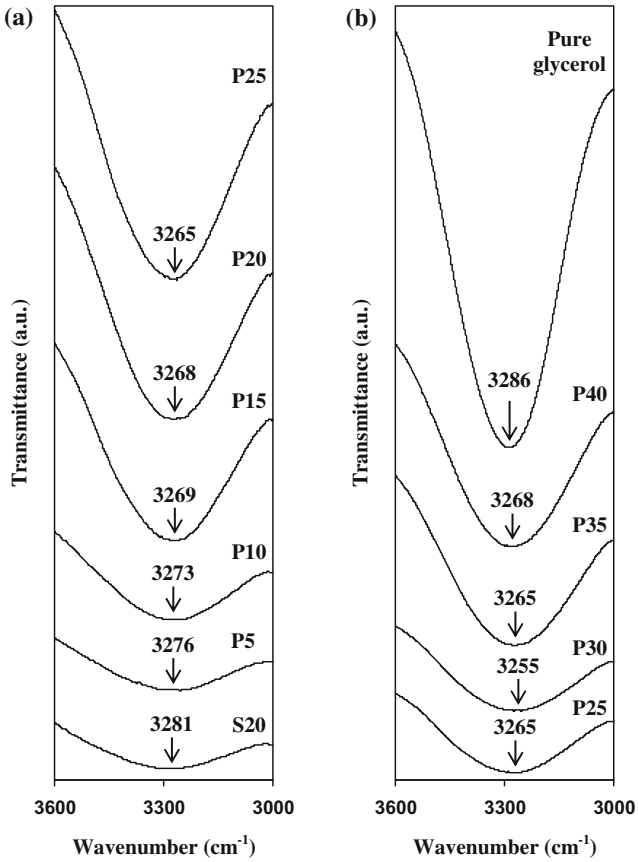

Fig. 3 FTIR spectra for **a** S20, P5, P10, P15, P20, and P25 and **b** P25, P30, P35, P40, and pure glycerol in the wavenumber region of 3000–3600 cm^{-1}

that more ions interact with the oxygen atom in anhydroglucose ring of starch. There is also possible hydrogen bonding between glycerol and starch in this region.

FTIR spectra of electrolytes in the IL-based system in the hydroxyl band region are shown in Fig. 5a. On addition of 5 wt.% BmImCl, the hydroxyl band peak shifts from 3255 to 3272 cm^{-1}. The hydroxyl band peak is observed to shift up to 3292 cm^{-1} as the BmImCl content increases to 18 wt.%. Another proof can be observed by the shifting of the peak of anhydroglucose ring of O–C stretch as shown in Fig. 5b. From a report by Sim et al. [35], the addition of ionic liquid into polymer-salt complex increases the amount of free ions. According to the authors, the cations from ionic liquid can coordinate at the polar atoms of polymer host. Thus, from Fig. 5, it can be indicated that the cation ($BmIm^+$) of BmImCl interacts with the oxygen atom of polymer. This result shows that ionic liquid can provide ions which can lead to the increase in conductivity as has been reported in the literature [35, 45, 46].

Room temperature conductivity

In the salted system, the incorporation of 20 wt.% $Mg(C_2H_3O_2)_2$ has maximized the room temperature conductivity to $(2.44 \pm 0.37) \times 10^{-8}$ S cm^{-1} as shown in Fig. 6a. The increase in conductivity as the salt content increases to 20 wt.% is attributed to the increase in the number of mobile charge carriers [23]. On addition of 25 wt.% $Mg(C_2H_3O_2)_2$, the conductivity decreases to $(7.82 \pm 1.30) \times 10^{-9}$ S cm^{-1} and further decreases to $(4.01 \pm 0.65) \times 10^{-9}$ S cm^{-1} with addition of 30 wt.% $Mg(C_2H_3O_2)_2$. This phenomenon is attributed to the aggregation of the ions, leading to the formation of ion clusters, thus decreasing the number of mobile charge carriers [47]. Different amounts of glycerol were added to the highest conducting electrolyte in the salted system in order to enhance the conductivity. From Fig. 6b, as the glycerol content increases to 30 wt.%, the room temperature conductivity is enhanced to $(2.60 \pm 0.42) \times 10^{-6}$ S cm^{-1}. Plasticization using glycerol has created alternative pathways for ion conduction leading to conductivity enhancement [48]. Besides, the addition of glycerol promotes ion dissociation which decreases the formation of ion aggregates and increases the number of mobile charge carriers. This phenomenon enhances the conductivity. On addition of more than 30 wt.% glycerol, the decrease in conductivity may be caused by the formation of linkages between the molecules of plasticizer causing the salt to recrystallize, resulting in a conductivity decrement [49,

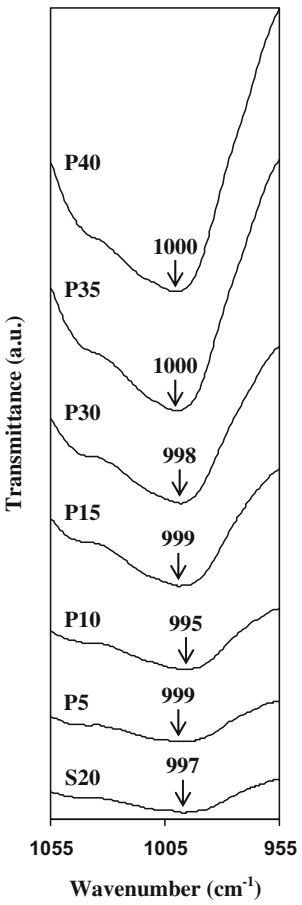

Fig. 4 FTIR spectra for selected electrolytes in the plasticized system in the wavenumber region of 955–1055 cm^{-1}

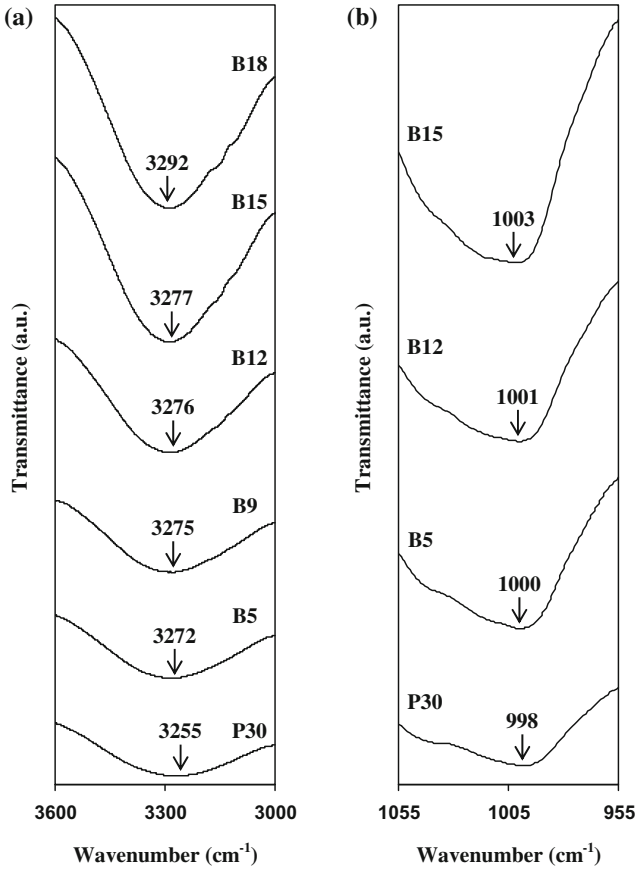

Fig. 5 FTIR spectra for electrolytes in the IL-based system in the wavenumber region of **a** 3000–3600 cm^{-1} and **b** 955–1055 cm^{-1}

50]. When too many plasticizer molecules exist within the electrolyte, the cations hardly coordinated at the polar atoms. This is because there is competition between the cations and the plasticizer molecules to interact with the polar atoms of polymer host or plasticizer molecules, thus increases the possibility of ion association which can decrease the conductivity.

To further enhance the conductivity, different amounts of BmImCl were added to the highest conducting electrolyte in the plasticized system. From Fig. 7, as the BmImCl content increases to 18 wt.%, the room temperature conductivity is enhanced to $(1.12 \pm 0.08) \times 10^{-5}$ S cm^{-1}. According to Kumar et al. [51], the addition of ionic liquid affects the properties of the polymer electrolytes in different ways. Generally, the conductivity enhancement can be related to the increase in free ions after the incorporation of ionic liquid. From the FTIR results, cations from the ionic liquid have interacted with the polar atoms of polymer. Thus, in the present electrolyte system, four ions, i.e., Mg^{2+} ion, the cation of the ionic liquid and the anions from both the salt and ionic liquid contribute to the ionic conductivity [52, 53]. The low viscosity of ionic liquid enhances the flexibility of the polymer backbone, thus increases the segmental motion [51]. Besides, the high dielectric constant of ionic liquid assists ion dissociation [54]. All these phenomena favour the ionic conductivity enhancement.

Dielectric analysis

The conductivity trend can be further verified by dielectric studies. Dielectric constant (ε_r) represents charge stored in a material [55]. The values of ε_r were calculated from the following equation:

$$\varepsilon_r = \frac{Zi}{\omega C_o \left(Z_r^2 + Z_i^2\right)} \tag{2}$$

where ω is angular frequency, C_o is vacuum capacitance, while Z_r and Z_i are real and imaginary parts of impedance, respectively. From Fig. 8, it is observed that higher conducting electrolyte has the higher value of ε_r at all frequencies. The increasing charge stored in the electrolyte means that the number density of mobile ions has increased [55]. This phenomenon increases the conductivity. Reports from the literature showed that the dielectric

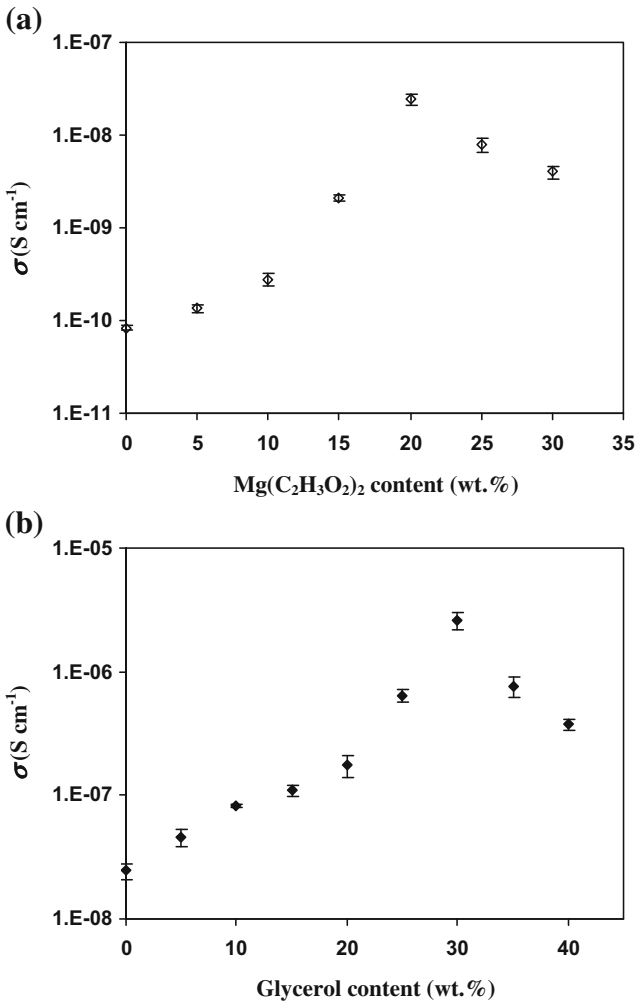

Fig. 6 Conductivity at room temperature for electrolytes in the **a** salted system and **b** plasticized system

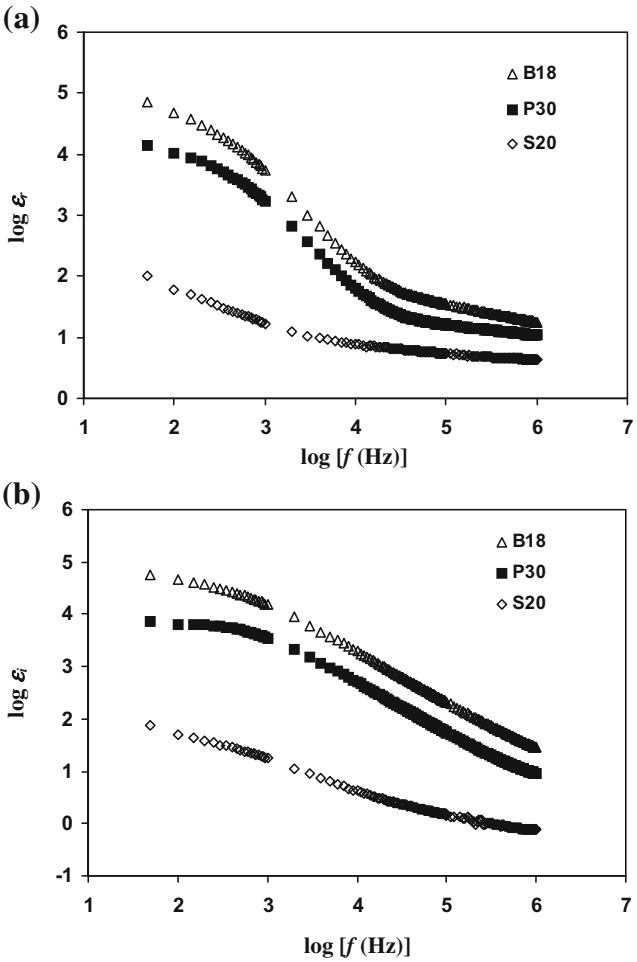

Fig. 8 Frequency dependence of **a** ε_r and **b** ε_i at room temperature for the highest conducting electrolyte in each system

constant result is in good agreement with the conductivity result [56–59]. The decrease in ε_r values with the increase in frequency is attributed to the electrode polarization effect [60]. As frequency increases, the periodic reversal of the electric field occurs so rapidly which disables the charge carriers from orienting themselves in the field direction, resulting in the decrease of ε_r [61].

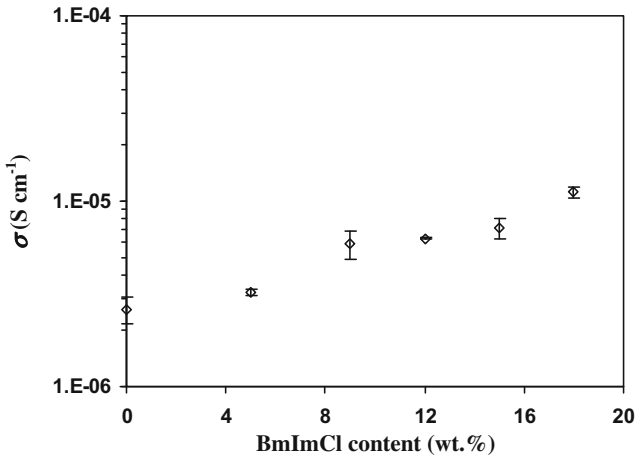

Fig. 7 Conductivity at room temperature for electrolytes in the IL-based system

The information of the relaxation phenomena of the highest conducting electrolyte in salted, plasticized, and IL-based systems is obtained from the plot of loss tangent (tan δ) as a function of frequency in Fig. 9. The value of tan δ was calculated using the following equation:

$$\tan\ \delta = \frac{\varepsilon_i}{\varepsilon_r} \tag{3}$$

The maximum of tan δ (tan δ_{max}), which represents the relaxation peak, is located at a higher frequency for the higher conducting electrolyte. The relaxation time (t_r) for each electrolyte was obtained from the relation as follows:

$$t_r \omega_{peak} = 1 \tag{4}$$

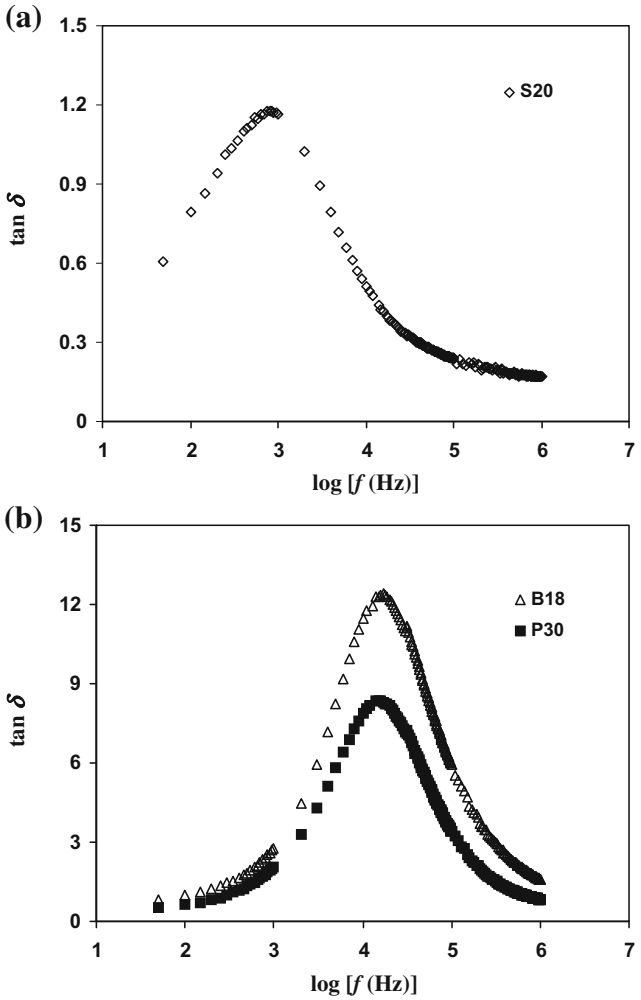

Fig. 9 The dependence of tan δ on frequency for **a** S20 and **b** P30 and B18 at room temperature

where ω_{peak} is the angular frequency of the relaxation peak. The occurrence of relaxation time is the result of the efforts carried out by ionic charge carriers to follow the change of the direction of the applied field [62]. The values of t_r for the electrolytes are presented in Table 4. The highest conducting electrolyte (B18) possesses the lowest t_r value of 9.36×10^{-6} s. Other reports also show that the higher conducting electrolytes have the lower values of t_r [44, 62, 63].

The distribution of relaxation times can be described by Kohlrausch-Williams-Watts law [64]:

$$\phi(t) = \exp\left[-\left(\frac{t}{t_r}\right)^{\beta}\right] \tag{5}$$

Table 4 Relaxation time of the highest conducting electrolyte in each system at room temperature

Sample	t_r (s)
S20	1.87×10^{-4}
P30	1.06×10^{-5}
B18	9.36×10^{-6}

where $\phi(t)$ describes the time evolution of the electric field within a material and β is the Kohlrausch exponent. In the present work, the values of β for S20, P30, and B18 electrolytes at room temperature are determined from the full width at half maximum (FWHM) of the normalized plot of tan δ/(tan δ)$_{max}$ against f/f_{max} in Fig. 10 using the following equation:

$$\beta = \frac{1.14}{\text{FWHM}} \tag{6}$$

For a typical Debye peak, the value of FWHM is 1.14 decades, which gives $\beta = 1$ for Debye relaxation [65, 66]. For a practical solid electrolyte, the value of β is less than 1 [67]. It is found that the values of β for S20, P30, and B18 electrolytes at room temperature are 0.58, 0.85, and 0.83, respectively. Since the values of β are lower than 1, it can be inferred that the relaxation deviates from Debye relaxation.

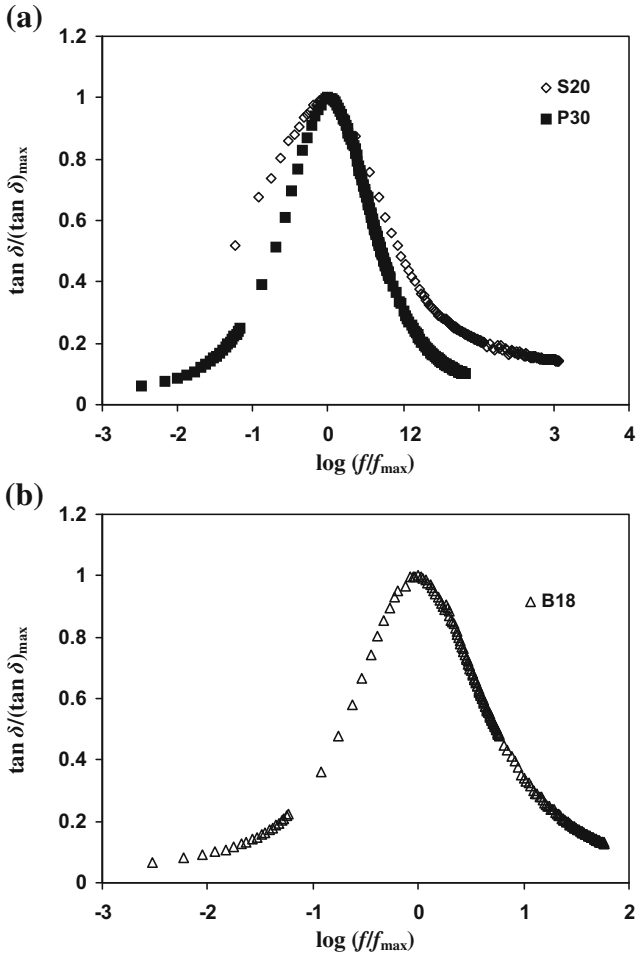

Fig. 10 Normalized plot of tan δ/(tan δ)$_{max}$ against f/f_{max} for **a** S20 and P30 and **b** B18 at room temperature

The real part and imaginary part of electrical modulus were calculated using

$$M_r = \frac{\varepsilon_r}{(\varepsilon_r^2 + \varepsilon_i^2)} \quad (7)$$

$$M_i = \frac{\varepsilon_i}{(\varepsilon_r^2 + \varepsilon_i^2)} \quad (8)$$

where M_r and M_i are real and imaginary parts of electrical modulus, respectively. Figure 11a shows the variation of M_r with frequency for the highest conducting electrolyte in each system at room temperature. The values of M_r increase as the frequency increases, but no definitive peaks appear in the M_r plots. The same result has been reported by Shukur et al. [68] for chitosan-polyethylene oxide (PEO)-ammonium nitrate (NH_4NO_3) system. Figure 11b shows the variation of M_i with frequency for the highest conducting electrolyte in each system at room temperature. A peak is observed in the M_i plot of S20 electrolyte indicating that the electrolyte is an ionic conductor [69]. The long tail of small values at lower frequencies in the M_i plots of P30 and B18 electrolytes is mainly due to high capacitance values which associated with the electrode, as a result of accumulation of charge carriers at the electrode-electrolyte interfaces [7, 70, 71].

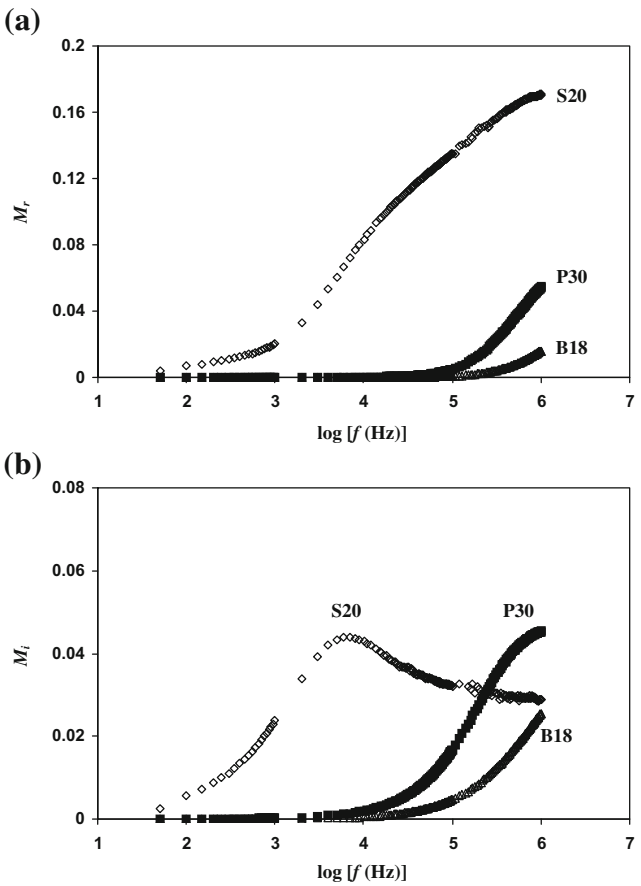

Fig. 11 The dependence of **a** M_r and **b** M_i on frequency for the highest conducting electrolyte in each system at room temperature

Transference number analysis

To detect the type of charge carriers in the polymer electrolytes, the transference number measurements were carried out. By sandwiching the electrolyte with charge carrier transparent electrodes, transference number of the charge carrier can be known from the ratio of steady-state current (I_{ss}) to the initial current (I_i). According to Kufian et al. [72], electrons are transparent to the ion blocking stainless steel electrodes. Thus, in the present work, stainless steels were used as the electrodes for the determination of transference number of electron (t_e). By knowing t_e, the value of t_{ion} of the electrolytes was calculated using

$$t_{ion} = 1 - t_e \quad (9)$$

Or

$$t_{ion} = \frac{I_i - I_{ss}}{I_i} \quad (10)$$

If ions are the dominant charge carriers, the current flows through the electrode will decrease rapidly with time, while if electrons are dominant, the current would not decrease with time [1, 33, 73]. The plots of polarization current against time for B18 electrolyte is shown in Fig. 12. The current is observed to decrease rapidly initially, before being saturated at 2.3 μA. This result shows that the electrolyte is an ionic conductor. The value of t_{ion} for B18 electrolyte is 0.92, further evidences that ions are the dominant charge carriers. The t_{ion} values for other magnesium ion conducting solid polymer electrolytes [74–76] have been reported to be >0.90, which is comparable with the present result.

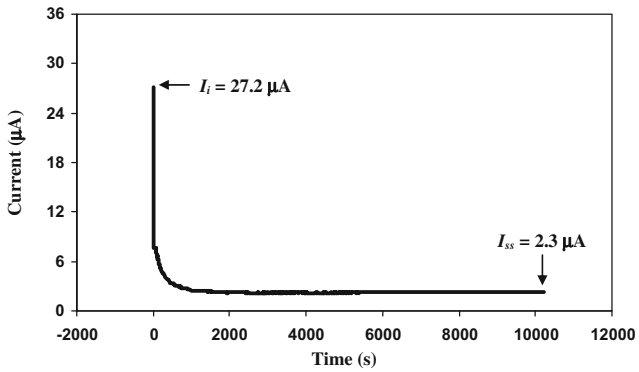

Fig. 12 Transference number of B18 electrolyte using stainless steel electrodes

Conclusions

Potato starch doped with $Mg(C_2H_3O_2)_2$-based electrolytes was successfully prepared via solution cast technique. FTIR analysis proved the interaction between the electrolyte materials. In the salted system, the electrolyte with 20 wt.% $Mg(C_2H_3O_2)_2$ (S20) has a conductivity of $(2.44 \pm 0.37) \times 10^{-8}$ S cm^{-1}. In the plasticized system, the addition of 30 wt.% glycerol (P30) has increased the conductivity to $(2.60 \pm 0.42) \times 10^{-6}$ S cm^{-1}. In the ionic liquid-based system, the addition of 18 wt.% BmImCl (B18) has further enhanced the conductivity to $(1.12 \pm 0.08) \times 10^{-5}$ S cm^{-1}. Dielectric analysis verified the conductivity result. The relaxation time (t_r) of electrolytes was determined from the loss tangent (tan δ) plot where higher conducting electrolyte has lower t_r value. Scaling of tan δ showed that the ionic relaxation was non-Debye type. From transference number measurement of B18 electrolyte, ions were found to be the dominant charge carriers with t_{ion} of 0.92.

Acknowledgments The authors thank the Malaysian Ministry of Higher Education for the Fundamental Research Grant Scheme (FRGS) support (Grant no: FP009-2015A).

References

1. Shukur MF, Kadir MFZ (2015) Hydrogen ion conducting starch-chitosan blend based electrolyte for application in electrochemical devices. Electrochim Acta 158:152–165
2. Sudhakar YN, Selvakumar M (2012) Lithium perchlorate doped plasticized chitosan and starch blend as biodegradable polymer electrolyte for supercapacitors. Electrochim Acta 78:398–405
3. Ng LS, Mohamad AA (2006) Protonic battery based on a plasticized chitosan-NH_4NO_3 solid polymer electrolyte. J Power Sources 163:382–385
4. Espindola-Gonzalez A, Martinez-Hernandez AL, Fernandez-Escobar F, Castano VM, Brostow W, Datashvili T, Velasco-Santos C (2011) Natural-synthetic hybrid polymers developed via electrospinning: the effect of PET in chitosan/starch system. Int J Mol Sci 12:1908–1920
5. Kumar SA, Vivek D, Vandana A (2012) Role of natural polymers used in floating drug delivery system. J Pharm Sci Innov 1:11–15
6. Raphael E, Avellaneda CO, Manzolli B, Pawlicka A (2010) Agar-based films for application as polymer electrolytes. Electrochim Acta 55:1455–1459
7. Khiar ASA, Arof AK (2010) Conductivity studies of starch-based polymer electrolytes. Ionics 16:123–129
8. Teramoto N, Motoyama T, Mosomiya R, Shibata M (2003) Synthesis, thermal properties, and biodegradability of propyl-etherified starch. Eur Polym J 39:255–261
9. Ramesh S, Liew C-W, Arof AK (2011) Ion conducting corn starch biopolymer electrolytes doped with ionic liquid 1-butyl-3-methylimidazolium hexafluorophosphate. J Non-Cryst Solids 357: 3654–3660
10. Tiwari T, Pandey K, Srivastava N, Srivastava PC (2011) Effect of glutaraldehyde on electrical properties of arrowroot starch + NaI electrolyte system. J Appl Polym Sci 121:1–7
11. Zhong F, Yokoyama W, Wang Q, Shoemaker CF (2006) Rice starch, amylopectin, and amylose: molecular weight and solubility in dimethyl sulfoxide-based solvents. J Agric Food Chem 54:2320–2326
12. Koganti N, Mitchell JR, Ibbett RN, Foster TJ (2011) Solvent effects on starch dissolution and gelatinization. Biomacromolecules 12: 2888–2893
13. Koganti N, Mitchell J, Macnaughtan W, Hill S, Foster T (2015) Effect of granule organisation on the behaviour of starches in the NMMO (N-methyl morpholine N-oxide) solvent system. Carbohydr Polym 116:103–110
14. Shen J, Wang L, Men Y, Wu Y, Peng Q, Wang X, Yang R, Mahmood K, Liu Z (2015) Effect of water and methanol on the dissolution and gelatinization of corn starch in [MMIM][(MeO)HPO_2]. RSC Adv 5:60330–60338
15. Guohua Z, Ya L, Cuilan F, Min Z, Caiqiong Z, Zongdao C (2006) Water resistance, mechanical properties and biodegradability of methylated-cornstarch/poly(vinyl alcohol) blend film. Polym Degrad Stabil 91:703–711
16. Hejri Z, Seifkordi AA, Ahmadpour A, Zebarjad SM, Maskooki A (2013) Biodegradable starch/poly (vinyl alcohol) film reinforced with titanium dioxide nanoparticles. Int J Min Met Mater 20: 1001–1011
17. Gonzalez Z, Perez E (2002) Effect of acetylation on some properties of rice starch. Starch 54:148–154
18. Xu Y, Hanna MA (2005) Physical, mechanical, and morphological characteristics of extruded starch acetate foams. J Polym Environ 13:221–230
19. Ochubiojo EM, Rodrigues A (2012) Starch: from food to medicine. In: Valdez B (ed) Scientific, health and social aspects of the food industry. InTech, Rijeka, Croatia, pp. 355–380
20. Tiwari T, Srivastava N, Srivastava PC (2011) Electrical transport study of potato starch-based electrolyte system. Ionics 17:353–360
21. Kumar M, Tiwari T, Srivastava N (2012) Electrical transport behaviour of bio-polymer electrolyte system: potato starch + ammonium iodide. Carbohydr Polym 88:54–60
22. Ibrahim S, Yassin MM, Ahmad R, Johan MR (2011) Effects of various $LiPF_6$ salt concentrations on PEO-based solid polymer electrolytes. Ionics 17:399–405
23. Noor ISM, Majid SR, Arof AK, Djurado D, Neto SC, Pawlicka A (2012) Characteristics of gellan gum-$LiCF_3SO_3$ polymer electrolytes. Solid State Ionics 225:649–653
24. Johansson JP (1998) Conformations and vibration in polymer electrolytes. Uppsala University, Sweden, Thesis Dissertation
25. Johari NA, Kudin TIT, Ali AMM, Yahya MZA (2011) Effects of TiO_2 on conductivity performance of cellulose acetate based polymer gel electrolytes for proton batteries. Mater Res Innov 15:S229–S231
26. Alves RD, Rodrigues LC, Andrade JR, et al. (2013) Study and characterization of a novel polymer electrolyte based on agar doped with magnesium triflate. Mol Cryst Liq Cryst 570:1–11
27. Shukur MF, Ithnin R, Illias HA, Kadir MFZ (2013) Proton conducting polymer electrolyte based on plasticized chitosan-PEO blend and application in electrochemical devices. Opt Mater 35:1834–1841
28. Kadir MFZ, Majid SR, Arof AK (2010) Plasticized chitosan-PVA blend polymer electrolyte based proton battery. Electrochim Acta 55:1475–1482
29. Kumar M, Sekhon SS (2002) Role of plasticizer's dielectric constant on conductivity modification of PEO-NH_4F polymer electrolytes. Eur Polym J 38:1297–1304
30. Rajendran S, Uma T (2001) FTIR and conductivity studies of PVC based polymer electrolyte systems. Ionics 7:122–125
31. Hu G, Chen J, Gao J (2009) Preparation and characteristics of oxidized potato starch films. Carbohydr Polym 76:291–298

32. Marcondes RFMS, D'Agostini PS, Ferreira J, Girotto EM, Pawlicka A, Dragunski DC (2010) Amylopectin-rich starch plasticized with glycerol for polymer electrolyte application. Solid State Ionics 181:586–591
33. Shukur MF, Kadir MFZ (2014) Electrical and transport properties of NH_4Br-doped cornstarch-based solid biopolymer electrolyte. Ionics 21:111–124
34. Liew C-W, Ramesh S, Arof AK (2014) Good prospect of ionic liquid based-poly(vinyl alcohol) polymer electrolytes for supercapacitors with excellent electrical, electrochemical and thermal properties. Int J Hydrogen Energ 39:2953–2963
35. Sim LN, Majid SR, Arof AK (2014) Effects of 1-butyl-3-methyl imidazolium trifluoromethanesulfonate ionic liquid in poly(ethyl methacrylate)/poly(vinylidenefluoride-co-hexafluoropropylene) blend based polymer electrolyte system. Electrochim Acta 123: 190–197
36. Ye Y-S, Rick J, Hwang B-J (2013) Ionic liquid polymer electrolytes. J Mater Chem A 1:2719–2743
37. Osman Z, Ghazali MIM, Othman L, Isa KBM (2012) AC ionic conductivity and DC polarization method of lithium ion transport in PMMA-$LiBF_4$ gel polymer electrolytes. Results Phys 2:1–4
38. Hema M, Selvasekerapandian S, Hirankumar G, Sakunthala A, Arunkumar D, Nithya H (2009) Structural and thermal studies of PVA:NH_4I. J Phys Chem Solids 70:1098–1103
39. Kadir MFZ, Aspanut Z, Majid SR, Arof AK (2011) FTIR studies of plasticized poly(vinyl alcohol)-chitosan blend doped with NH_4NO_3 polymer electrolyte membrane. Spectrochim Acta A 78:1068–1074
40. LN S (2014) PhD thesis. In: Investigation on PEMA/PVdF-HFP blend polymer electrolytes incorporated with carbonate-based plasticizers and imidazolium-based ionic liquids. University of Malaya, Kuala Lumpur, Malaysia
41. Stygar J, Zukowska G, Wieczorek W (2005) Study of association in alkali metal perchlorate-poly(ethylene glycol) monomethyl ether solutions by FT-IR spectroscopy and conductivity measurements. Solid State Ionics 176:2645–2652
42. Huang CB, Jeng R, Sain M, Saville BA, Hubbes M (2006) Production, characterization, and mechanical properties of starch modified by *Ophiostoma* spp. Bioresources 1:257–269
43. Yusof Y, Majid NA, Kasmani RM, Illias HA, Kadir MFZ (2014) The effect of plasticization on conductivity and other properties of starch/chitosan blend biopolymer electrolyte incorporated with ammonium iodide. Mol Cryst Liq Cryst 603:73–88
44. Shukur MF, Ithnin R, Kadir MFZ (2014) Electrical properties of proton conducting solid biopolymer electrolytes based on starch-chitosan blend. Ionics 20:977–999
45. Liew C-W, Ramesh S, Arof AK (2014) A novel approach on ionic liquid-based poly(vinyl alcohol) proton conductive polymer electrolytes for fuel cell applications. Int J Hydrogen Energy 39:2917–2928
46. Anuar NK, Subban RHY, Mohamed NS (2012) Properties of PEMA-$NH_4CF_3SO_3$ added to BMATSFI ionic liquid. Mater 5: 2609–2620
47. Ramya CS, Selvasekarapandian S, Savitha T, Hirankumar G, Angelo PC (2007) Vibrational and impedance spectroscopic study on PVP-NH_4SCN based polymer electrolytes. Physica B 393:11–17
48. Pawlicka A, Sabadini AC, Raphael E, Dragunski DC (2008) Ionic conductivity thermogravimetry measurements of starch-based polymeric electrolytes. Mol Cryst Liq Cryst 485:804–816
49. Johan MR, Ting LM (2011) Structural, thermal and electrical properties of Nano manganese-composite polymer electrolytes. Int J Electrochem Sci 6:4737–4748
50. Ramesh S, Arof AK (2000) Electrical conductivity studies of polyvinyl chloride-based electrolytes with double salt system. Solid State Ionics 136-137:1197–1200
51. Kumar Y, Hashmi SA, Pandey GP (2011) Lithium ion transport and ion-polymer interaction in PEO based polymer electrolyte plasticized with ionic liquid. Solid State Ionics 201:73–80
52. Ye H, Huang J, Xu JJ, Khalfan A, Greenbaum SG (2007) Li ion conducting polymer gel electrolytes based on ionic liquid/PVDF-HFP blends. J Electrochem Soc 154:A1048–A1057
53. Karmakar A, Ghosh A (2014) Structure and ionic conductivity of ionic liquid embedded PEO-$LiCF_3SO_3$ polymer electrolyte. AIP Adv 4:087112
54. Kumar Y, Pandey GP, Hashmi SA (2012) Gel polymer electrolyte based electrical double layer capacitors: comparative study with multiwalled carbon nanotubes and activated carbon electrodes. J Phys Chem C 116:26118–26127
55. Buraidah MH, Teo LP, Majid SR, Arof AK (2009) Ionic conductivity by correlated barrier hopping in NH_4I doped chitosan solid electrolyte. Physica B 404:1373–1379
56. Shukur MF, Majid NA, Ithnin R, Kadir MFZ (2013) Effect of plasticization on the conductivity and dielectric properties of starch-chitosan blend biopolymer electrolytes infused with NH_4Br. Phys Scripta T157:014051
57. Kadir MFZ, Arof AK (2011) Application of PVA-chitosan blend polymer electrolyte membrane in electrical double layer capacitor. Mater Res Innov 15:S217–S220
58. Aziz NA, Majid SR, Arof AK (2012) Synthesis and characterizations of phthaloyl chitosan-based polymer electrolytes. J Non-Cryst Solids 358:1581–1590
59. Shukur MF, Ibrahim FM, Majid NA, Ithnin R, Kadir MFZ (2013) Electrical analysis of amorphous corn starch-based polymer electrolyte membranes doped with LiI. Phys Scripta 88:025601
60. Mishra R, Rao KJ (1998) Electrical conductivity studies of poly (ethyleneoxide)-poly (vinylalcohol) blends. Solid State Ionics 106:113–127
61. Ali RM, Harun NI, Ali AMM, Yahya MZA (2011) Conductivity studies on plasticised cellulose acetate–ammonium iodide based polymer electrolytes. Mater Res Innov 15:S39–S42
62. Ramly K, Isa MIN, Khiar ASA (2011) Conductivity and dielectric behaviour studies of starch/PEO + x wt-%NH_4NO_3 polymer electrolyte. Mater Res Innov 15:S82–S85
63. Hashim MA, Khiar ASA (2011) Supercapacitor based on activated carbon and hybrid solid polymer electrolyte. Mater Res Innov 15: S63–S66
64. Williams G, Watts DC (1970) Non-symmetrical dielectric relaxation behaviour arising from a simple empirical decay function. Trans Faraday Soc 66:80–85
65. Idris NH, Senin HB, Arof AK (2007) Dielectric spectra of LiTFSI-doped chitosan/PEO blends. Ionics 13:213–217
66. Dutta P, Biswas S, De SK (2002) Dielectric relaxation in polyaniline-polyvinyl alcohol composites. Mater Res Bull 37: 193–200
67. Padmasree KP, Kanchan DK, Kulkarni AR (2006) Impedance and modulus studies of the solid electrolyte system $20CdI_2$-$80[xAg_2O$-$y(0.7V_2O_5$-$0.3B_2O_3)]$, where $1 \le x/y \le 3$. Solid State Ionics 177: 475–482
68. Shukur MF, Kadir MFZ, Ahmad Z, Ithnin R (2012) Dielectric studies of proton conducting polymer electrolyte based on chitosan/PEO blend doped with NH_4NO_3. Adv Mater Res 488-489:583–587
69. Ali AMM, Bahron H, Subban RHY, Kudin TIT, Yahya MZA (2009) Frequency dependent conductivity studies on PMMA-$LiCF_3SO_3$ polymer electrolytes. Mater Res Innov 13:285–287
70. Aziz SB, Abidin ZHZ, Arof AK (2010) Influence of silver ion reduction on electrical modulus parameters of solid polymer electrolyte based on chitosan-silver triflate electrolyte membrane. Express Polym Lett 5:300–310

71. Hema M, Selvasekarapandian S, Nithya H, Sakunthala A, Arunkumar D (2009) Structural and ionic conductivity studies on proton conducting polymer electrolyte based on polyvinyl alcohol. Ionics 15:487–491
72. Kufian MZ, Aziz MF, Shukur MF, et al. (2012) PMMA-LiBOB gel electrolyte for application in lithium ion batteries. Solid State Ionics 208:36–42
73. KS Y (2012) Characteristics of PMMA-grafted natural rubber polymer electrolytes. In: PhD thesis. University of Malaya, Kuala Lumpur, Malaysia
74. Polu AR, Kumar R, Rhee H-W (2015) Magnesium ion conducting solid polymer blend electrolyte based on biodegradable polymers and application in solid-state batteries. Ionics 21:125–132
75. Polu AR, Kumar R (2013) Ionic conductivity and discharge characteristic studies of PVA-$Mg(CH_3COO)_2$ solid polymer electrolytes. Int J Polym Mater 62:76–80
76. Polu AR, Kumar R (2012) Ion-conducting polymer electrolyte based on poly (ethylene glycol) complexed with $Mg(CH_3COO)_2$-application as an electrochemical cell. E-J Chem 9:869–874